A Virtual Space Model based on Torque Gradient of IPMSMs with Nonlinear Characteristics

Takumi Ohnuma[1]

[1] National Institute of Technology, Numazu College, Japan

***Abstract*-- This paper proposes a virtual space model of IPMSMs with nonlinear characteristics to improve torque control performances. The nonlinear torque including a reluctance component, magnetic saturation, spatial harmonics, and variation of the magnetic energy degrade control performances. To solve this problem, we propose a virtual space model, which is obtained by transforming current and voltage spaces with virtual vectors. The virtual vectors are defined by gradients of a torque map on the *d-q* current plane of IPMSMs. The proposed virtual space is suitable for torque control because the basis vectors are based on the torque map. We applied the virtual space model to a sensorless torque feedback control system to confirm the validity of the proposed model. As a result of a simulation, it is verified that the maximum torque response under a voltage limitation and the Maximum Torque Per Ampere control are achieved by the virtual space model.**

***Index Terms*-- Maximum Torque Control Reference Frame, Torque Feedback Control, Torque Gradient, Torque Map**

I. Introduction

In recent years, Interior Permanent Magnet Synchronous Motors (IPMSMs) have attracted attentions for their high-torque control performances and high-efficiency in various applications. IPMSMs have nonlinear torque characteristics due to saliency, magnetic saturation, spatial harmonics, and variation of magnetic energy, while they are designed for high-torque density and wide-range drives. Their nonlinear characteristics make the control models to realize high-torque control performances complicated. An accurate torque equation is needed to achieve the required control performances [1]. Various strategies based on Look-up tables [2] have been studied to solve this problem. To analyze the nonlinear torque characteristics including magnetic saturation, spatial harmonics, and variation of the magnetic energy, a torque-sensorless identification of IPMSM torque map is proposed in the reference [3]. According to the study, the torque map can be reconstructed from torque gradients on the *d-q* current plane. Through the gradient theorem, the torque map can be experimentally obtained without a torque sensor. Once a highly accurate torque map is obtained, it is possible to achieve a torque sensorless feedback control.

In reference [4], a control method for achieving maximum torque response based on Maximum Torque Control Reference Frame (*f-t* axes) is introduced. The *f-t* axes are defined by a direction parallel to the constant torque curves in the *d-q* current plane. While the current change in the *t*-axis achieves optimal torque response, the phase angle is influenced by motor parameters. Thus, a precise determination method for the phase angle becomes crucial in ensuring torque control performance. Additionally, it should be noted that the responsiveness cannot be adjusted during voltage saturation since it serves as a voltage limiter.

In this paper, we extend the concept of the Maximum Torque Control Reference Frame (*f-t* axes) to a virtual space model in both current and voltage spaces. First, basis vectors for the virtual space are derived by torque gradients and a virtual flux in the current space. Since the torque gradients are provided by a multivariable torque map, the proposed virtual model can be applied for nonlinear motors with a parameter variation. Then, we introduce a new definition of the Maximum Torque Control Reference Frame in the voltage space. Basis vectors for the voltage space are derived by transforming the virtual flux vector with an inductance matrix. The proposed model is then applied to a torque sensorless feedback control system to reasonably achieve a maximum torque response under current and voltage magnitude limitations. The *f-t* axes for voltage space are suitable for torque feedback control because time derivative of torque is formularized by the virtual vectors in the voltage space. The proposed torque feedback controllers can adjust the responsiveness of the *f*-axis current and the torque control independently.

II. Virtual Space Model based on Torque Gradients

A. Torque Gradient on Current Vector Space

First, we generally express the magnitude of motor torque per pole-pairs of IPMSMs as a function of two independent variables which are *d*- and *q*- axis currents, i_d and i_q.

$$\tau = \tau(i_d, i_q) \tag{1}$$

Although the equation (1) supposes two dimensions of the *d-q* axis currents in this paper, a general torque map can be extended to a multivariable function including a rotor position to express space harmonics.

Then, the gradient torque on the *d-q* current plane can be expressed as Eq. (2).

$$\boldsymbol{\nabla}\tau = \frac{\partial \tau}{\partial i_d}\boldsymbol{u_d} + \frac{\partial \tau}{\partial i_q}\boldsymbol{u_q} \tag{2}$$

Here, $\boldsymbol{u_d}$ and $\boldsymbol{u_q}$ are unit basis vectors in the *d-q* coordinate system. As shown in Fig.1, the torque gradients are the variable vectors depending on the *d-q* currents.

Now, we define a virtual magnetic flux vector $\boldsymbol{\Psi_m}$ as Eq. (3) since a physical dimension of torque/current is magnetic flux.

$$\boldsymbol{\Psi_m} = \boldsymbol{J}^T \boldsymbol{\nabla} \tau \tag{3}$$

Here, the matrix $\boldsymbol{J}$ is the 90-degree rotation matrix as shown in Eq. (4).

$$\boldsymbol{J} = \begin{pmatrix} 0 & -1 \\ 1 & 0 \end{pmatrix} \tag{4}$$

As shown in Fig. 2(a), we define bases of the virtual space to transform the current vectors by unit-direction vectors, $\boldsymbol{u_f}$ and $\boldsymbol{u_t}$, in the direction of the virtual flux $\boldsymbol{\Psi_m}$ and the torque gradient $\boldsymbol{\nabla}\tau$, respectively. That is, the

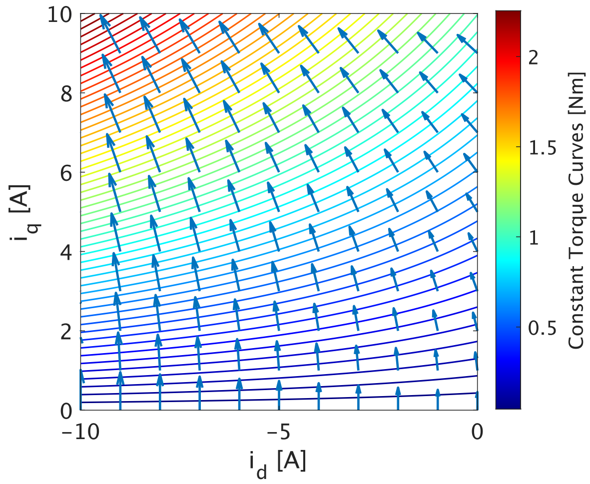

Fig. 1. An example of torque gradients on a current space.

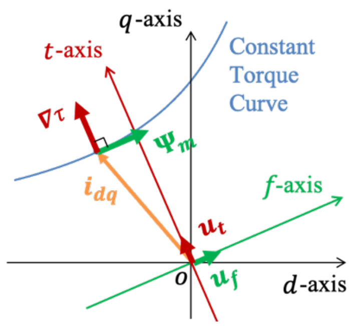

(a) Current space

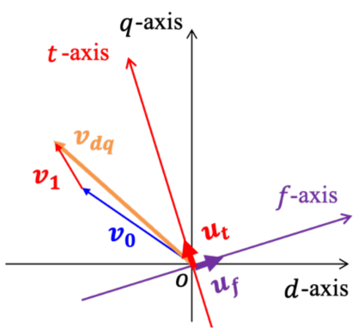

(b) Voltage space

Fig. 2. Maximum Torque Control Reference Frames.

basis vectors for the current space can be expressed as Eq. (5).

$$\boldsymbol{u_f} = \frac{\boldsymbol{\Psi_m}}{|\boldsymbol{\Psi_m}|}, \qquad \boldsymbol{u_t} = \frac{\boldsymbol{\nabla}\tau}{|\boldsymbol{\nabla}\tau|} \tag{5}$$

The Maximum Torque Control Reference Frame [4], which is denoted as *f-t* axes, can be defined by these basis vectors because the *f*-axis is aligned parallel to the constant torque curves on the *d-q* current space. Figure 3 shows an example of the mapping of torque from the *d-q* space to the *f-t* space. The *f-t* axis currents are calculated by inner products of the *d-q* axis current vectors $\boldsymbol{i_{dq}}$ and the basis vectors $\boldsymbol{u_f}$, $\boldsymbol{u_t}$ as follows:

$$i_f = \boldsymbol{u_f} \cdot \boldsymbol{i_{dq}}, \qquad i_t = \boldsymbol{u_t} \cdot \boldsymbol{i_{dq}}. \tag{6}$$

It is found that the Maximum Torque Per Ampere (MTPA) current locus is transformed onto the *t*-axis, since the *f*-axis current component is zero when the MTPA control is achieved.

B. Maximum Torque Control Reference Frame on Voltage Space

Generally, when a voltage source inverter is used to control an IPMSM, the manipulated variable is the voltage. Therefore, in this section, we consider the Maximum Torque Control Reference Frame in the voltage space in order to deal with the voltage manipulated variable saturation problem. First, the *d-q* voltage vector is divided into two components, which are the terms of the steady state $\boldsymbol{v_0}$ and the transient state $\boldsymbol{v_1}$ as Eq. (7).

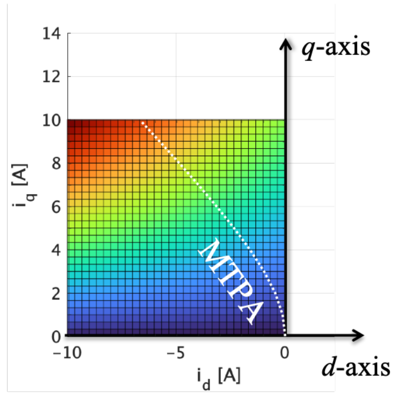

(a) on the *d-q* current plane

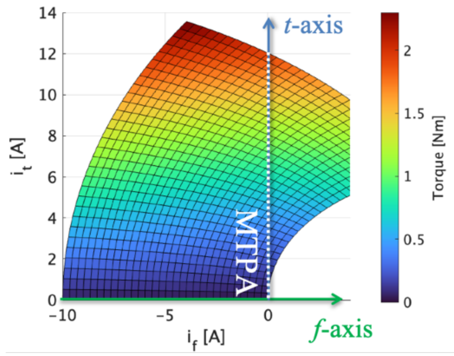

(b) on the *f-t* current plane

Fig. 3. Mapping of torque on current planes.

$$\boldsymbol{v}_{dq} = \boldsymbol{v}_0 + \boldsymbol{v}_1 = \boldsymbol{v}_0 + p\boldsymbol{L}_{dq}\boldsymbol{i}_{dq} \tag{7}$$

Here, according to an inductance model, the transient voltage v_1 is supposed to be generated by a change of the current vector with time. The "p" is the differential operator with respect to time. The inductance matrix $\boldsymbol{L}_{dq}$ includes cross-coupling components as follows:

$$\boldsymbol{L}_{dq} = \begin{pmatrix} L_d & L_{dq} \\ L_{qd} & L_q \end{pmatrix}. \tag{8}$$

When a current vector changes with time, time derivative of torque is expressed as follows:

$$p\tau = \frac{d\tau}{dt} = (\boldsymbol{\nabla}\tau) \cdot (p\boldsymbol{i}_{dq}) \tag{9}$$

The time derivative of the torque in Eq. (9) can be transformed using the virtual magnetic flux $\boldsymbol{\Psi}_m$ in Eq. (3) and the transient voltage $\boldsymbol{v}_1$ in Eq. (7), resulting in Eq. (10).

$$p\tau = \left(\boldsymbol{J}\frac{\boldsymbol{L}_{dq}}{|\boldsymbol{L}_{dq}|}\boldsymbol{\Psi}_m\right) \cdot \boldsymbol{v}_1 = (\boldsymbol{J}\boldsymbol{\Gamma}_m) \cdot \boldsymbol{v}_1 \tag{10}$$

Here, the $\boldsymbol{\Gamma}_m$ is a virtual vector on the voltage space, which is defined by the virtual magnetic flux $\boldsymbol{\Psi}_m$ and the inductance matrix, as shown in Eq. (11).

$$\boldsymbol{\Gamma}_m = \frac{\boldsymbol{L}_{dq}}{|\boldsymbol{L}_{dq}|}\boldsymbol{\Psi}_m \tag{11}$$

As shown in Fig. 2(b), the *f*-*t* axes in the voltage space are defined on the basis of the unit direction vector of the virtual vector $\boldsymbol{\Gamma}_m$ and its orthogonal vector $(\boldsymbol{u}_f, \boldsymbol{u}_t)$ as shown in Eq. (12).

$$\boldsymbol{u}_f = \frac{\boldsymbol{\Gamma}_m}{|\boldsymbol{\Gamma}_m|}, \qquad \boldsymbol{u}_t = \boldsymbol{J}\boldsymbol{u}_f \tag{12}$$

That is, by mapping the current space using the inductance matrix in Eq. (8), the *f*-*t* axes on the voltage space can be obtained. Assuming a diagonal inductance matrix with no cross-coupling for sake of simplicity, this transformation matrix scales the aspect ratio of the coordinates by the saliency ratio L_q/L_d. The *f*-*t* axis voltages are calculated by inner products of the *d*-*q* axis voltage vectors $\boldsymbol{v}_{dq}$ and the basis vectors for voltage space in Eq. (12) as follows:

$$v_f = \boldsymbol{u}_f \cdot \boldsymbol{v}_{dq}, \qquad v_t = \boldsymbol{u}_t \cdot \boldsymbol{v}_{dq}. \tag{13}$$

C. Torque Feedback Control System for the Virtual Space Model

To design the torque feedback control based on the Eq. (10), a plant model in the virtual space is constructed as shown in Fig. 4. First, the voltage vector is divided into two components, which are the steady state $\boldsymbol{v}_0$ and the transient state $\boldsymbol{v}_1$. Second, the basis vectors in the voltage space are set as shown in Eq. (12). Third, the *t*-axis components for $\boldsymbol{v}_0$ and $\boldsymbol{v}_1$ are calculated by the inner product with $\boldsymbol{u}_t$. Then, according to Eq. (10), the plant model can be expressed by Eq. (14).

$$p\tau = |\boldsymbol{\Gamma}_m| v_{1t} \tag{14}$$

Here, v_{1t} is the *t*-axis component of the $\boldsymbol{v}_1$ vector.

As shown in Fig. 4, the *t*-axis components of the voltage vectors $\boldsymbol{v}_0$ and $\boldsymbol{v}_1$ can be regarded as an input and a disturbance to the plant, respectively. Therefore, putting the proportional control with the disturbance compensation for the torque feedback controller at the input of the plant, the closed-loop transfer function become a simple first-order lag system. The torque control is realized by only the *t*-axis voltage independently from the *f*-axis component in the proposed control system.

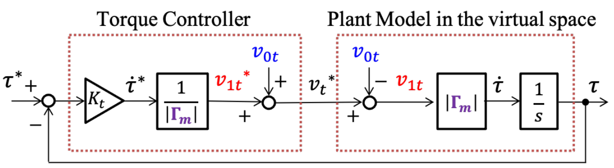

Fig. 4. Torque feedback control system.

III. Simulation

A. Simulation Conditions

As shown in Fig. 5, we constructed a Maximum Torque Control system in MATLAB/Simulink to confirm the validity of the proposed model. The torque step response under the voltage limit was tested and evaluated the response time. The tested machine is an IPMSM of 500 [W]. The resistance, EMF constant, *d*- and *q*-axis inductances are 0.55 [Ω], 0.104 [V/(rad/s)], 4.15 [mH], and 16.74 [mH], respectively. The *f*-axis current and the torque control gains are 5 [rad/s] and 10,000 [rad/s], respectively. The torque command is step-up to 0.5 [Nm] at 1 [ms] from the simulation start. The torque control is set to high gain to evaluate the torque response under the voltage saturation. The limit voltage magnitude is set to 100 [V]. The magnetic saturation and cross-coupling inductances are ignored in this simulation. The rotor speed is set to the constant at 1,000 [min^{-1}].

B. Simulation Results

Figures 6, 7, and 8 show the simulation results of a step torque response under voltage saturation. The torque is linearly rising to the command of 0.5 [Nm] without overshoot. The *d*-*q* axis currents are gradually converged toward the MTPA operating point after settling the torque. The voltage amplitude is limited within the voltage limit while the torque is rising. From the result as shown in Fig. 7(b), it was confirmed that the *t*-axis voltage component preferentially used to rapidly increase the torque. As shown in Fig. 8, since the control gain for the *f*-axis loop is set low enough, the *f*-axis current gradually converged to zero for the MTPA control after the torque has settled.

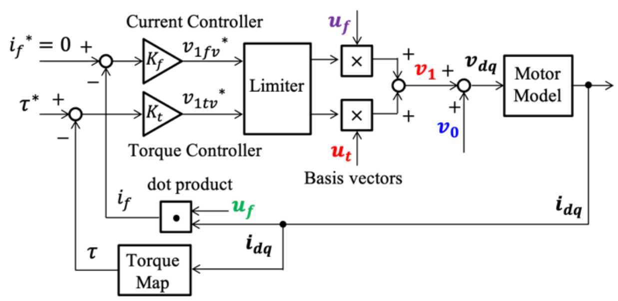

Fig. 5. Simulation control block.

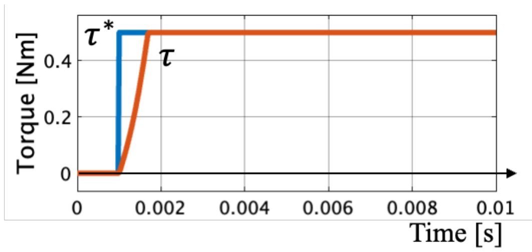

(a) Torque waveforms

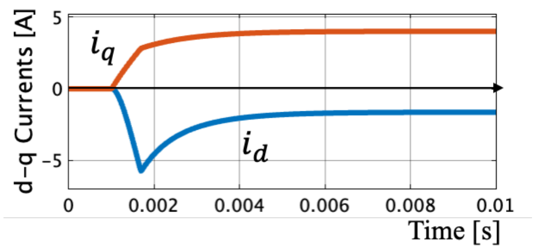

(b) *d-q* current waveforms

Fig. 6. Simulation results of torque step response.

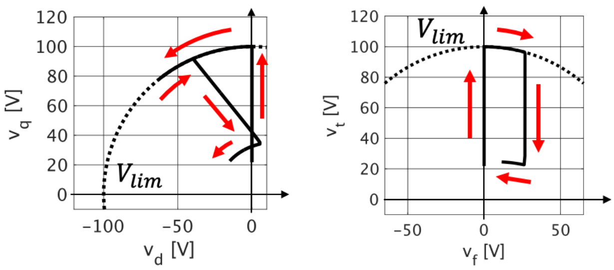

(a) on the *d-q* voltage plane (b) on the *f-t* voltage plane

Fig. 7. Voltage loci.

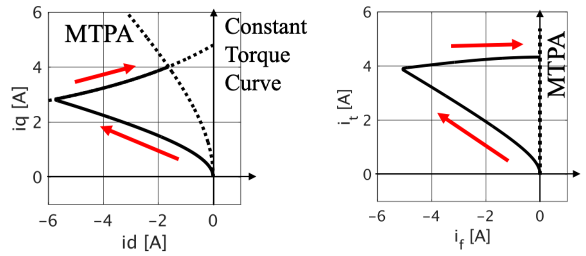

(a) on the *d-q* current plane (b) on the *f-t* current plane

Fig. 8. Current loci.

The transient *f*-axis current in the negative direction helps to improve the torque response in terms of the field weakening effect, while the MTPA control is suitable for efficiency at steady state. We confirmed that the proposed method effectively achieves Maximum Torque Response and the MTPA controls.

IV. Conclusions

This paper proposed a virtual space model for IPMSMs with nonlinear torque characteristics to improve the torque control performances. We introduced virtual vectors defined by torque gradients which are suitable for maximum torque controls. The validity of the proposed model was confirmed by simulations. The spatial harmonics will be considered, and the experimental verification with actual machines will be carried out in our future work.

References

[1] N. Kawamura, et al.: "A Method to Design the Controller for Single Pulse Mode Torque Feedback Control System of IPMSM", *IEEJ, Journal of Ind. Appl.*, Vol.11, No.4, pp.582-593, 2022

[2] E. Trancho, et al.: "IPMSM Torque Control Strategies based on LUTs and VCT feedback for Robust Control under Machine Parameter Variations", *42nd Annual Conf. of the IEEE Ind. Elec. Society*, pp.2833-2838, 2016

[3] H. -J. Cho, et. al, "Torque-Sensorless Identification of IPMSM Torque Map," *2021 IEEE ECCE*, pp. 4661-4667, 2021

[4] Y. Makaino, et al.: "Maximum Torque Response Control based on Maximum Torque Control Frame", *IEEJ Journal of Ind. Appl.*, Vol.3, No.3, pp.221-226, 2014